

An aluminum nitride photoconductor for X-ray detection*

Wang Xinjian(王新建)^{1,2}, Song Hang(宋航)^{1,†}, Li Zhiming(李志明)¹, Jiang Hong(蒋红)¹,
Li Dabing(黎大兵)¹, Miao Guoqing(缪国庆)¹, Chen Yiren(陈一仁)¹, and Sun Xiaojuan(孙晓娟)¹

¹State Key Laboratory of Luminescence and Applications, Changchun Institute of Optics, Fine Mechanics and Physics, Changchun 130033, China

²Graduate University of the Chinese Academy of Sciences, Beijing 100039, China

Abstract: An AlN photoconductor for X-ray detection has been fabricated, and its response to X-ray irradiation intensity is studied. The photoconductor has a very low leakage current, less than 0.1 nA at an applied voltage of 100 V in the absence of X-ray irradiation. The photocurrent measurement results clearly reveal that the photocurrent is proportional to the square root of the X-ray irradiation intensity, and under relatively high irradiation the photocurrent can reach values one order of magnitude larger than the dark current when a voltage of 100 V is applied across the AlN photoconductor. By using the ABC model the dependence of the photocurrent on the X-ray irradiation intensity is analyzed, and a reasonable interpretation of the physical mechanism is obtained.

Key words: AlN photoconductor; X-ray detection; recombination

DOI: 10.1088/1674-4926/33/10/103002

EEACC: 2520

1. Introduction

Compared with other semiconductors, AlN has a number of excellent physical and chemical properties. AlN, a direct transition-type semiconductor with a band gap of 6.2 eV at room temperature, shows high electrical resistivity, good thermal stability, and good radiation resistance^[1,2]. These properties make AlN a very attractive material for the fabrication of X-ray detectors. The wide band gap gives a relatively high electron-hole pair generation energy of about 15.5 eV, which implies that the charge signal amplitude of AlN X-ray detectors is four times smaller than that of silicon (Si) X-ray detectors^[3]. Furthermore, the high electrical resistivity makes the leakage current almost negligible, and the AlN X-ray detectors can reach a signal/noise ratio greatly higher than that of the Si X-ray detectors^[4]. Most importantly, the good thermal stability and radiation resistance allows the operation at a high temperature and harsh radiation environment, and the AlN X-ray detectors can still maintain the sub-keV spectral resolution at hard X-ray wavelengths^[5]. Unfortunately, due to the lack of appropriate substrates, AlN films are usually grown on sapphire or SiC substrates. The lattice and thermal mismatch between these substrates and AlN can cause a large number of dislocations in the heteroepitaxial AlN films, even various kinds of technologies such as the selective epitaxial growth and lateral overgrowth have been used to reduce the dislocations^[2]. These dislocations, in addition to the native defects and unintentionally incorporated background impurities, such as nitrogen vacancies (V_N) and oxygen (O), can cause many trapping centers in the heteroepitaxial AlN films to increase the trapping and reduce the mobilities, i.e., one or both charge carriers have low mobility μ or short lifetime τ . Small mobility-lifetime products $\mu\tau$ result in short drift lengths, which in turn limit the maximum photocurrent gain of the AlN X-ray detec-

tors. Indeed, to the best of our knowledge there has been limited work done concerning the feasibility of X-ray detection by exploiting the AlN detectors.

In the present work, the feasibility of X-ray detection by exploiting the AlN photoconductor is demonstrated, and its response to the X-ray irradiation intensity is investigated in details.

2. Experiment

A 1- μm -thick unintentionally doped wurtzite AlN film was grown by metal organic vapor phase epitaxy (MOVPE) on a polished optical-grade C-face (0001) sapphire substrate. Trimethylaluminum (TMAI) and ammonia (NH_3) were used as aluminum (Al) and nitrogen (N) sources, respectively. The carrier gas was hydrogen (H_2) and nitrogen (N_2), and the growth pressure was kept at 110 mbar. An AlN buffer layer was first grown on the sapphire substrate at a temperature of 500 °C, which was greatly lower than the growth temperature of the AlN epitaxial layer. Once the buffer layer was grown, the temperature was raised to 1150 °C to grow the AlN epitaxial layer. After the AlN epitaxial layer was grown, the whole film was diced into $10 \times 10 \text{ mm}^2$ squares. Before preparing for the fabrication of AlN photoconductors, all films were cleaned sequentially in an ultrasonic bath with acetone, alcohol and deionized water for 15 min in order to remove any organic and inorganic surface contamination, and then they were dried thoroughly using high purity N_2 . Finally, Ti/Al (20 nm/250 nm) interdigitated electrodes were formed by optical lithography and electron beam evaporation, and subsequently these photoconductors were annealed at a temperature of 600 °C for 7 min in N_2 atmosphere in order to decrease the electrical contact resistances. The length and width of the fingers were 100 μm and 5 μm , and the gap between two fingers was also 5 μm .

* Project supported by the National Natural Science Foundation of China (Nos. 51072196, 51072195).

† Corresponding author. Email: songh@ciomp.ac.cn

Received 4 March 2012, revised manuscript received 18 April 2012

© 2012 Chinese Institute of Electronics

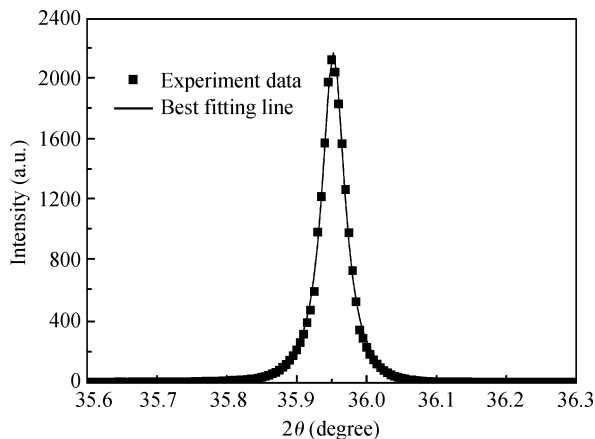


Fig. 1. XRD patterns of the grown AlN film.

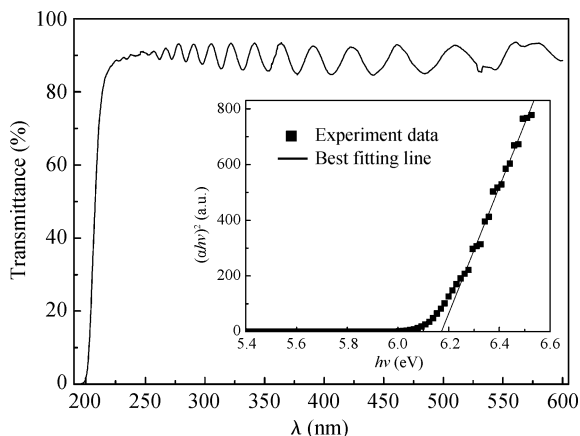


Fig. 2. Optical transmittance spectra of the grown AlN film. Inset is the determination of the band gap of the grown AlN film.

The crystal quality of the AlN film was examined by an X-ray diffractometer (XRD) and its optical absorption properties were characterized by a dual beam scanning spectrophotometer (UV-3101PC, Shimadzu, Japan). The Cu anode X-ray tube equipped on the X-ray diffractometer (D8Focus, Bruker, Germany) was used as the X-ray source, and its power could be changed from 10 kV × 0 mA to 40 kV × 40 mA. The photocurrent and dark current measurements for the AlN photoconductors were carried out by source measurement units (KEITHLEY model 237, America).

3. Results and discussion

The XRD measurements in $\theta/2\theta$ configuration are used to characterize the crystal quality of the AlN film, and the result for the (0002) plane scan is shown in Fig. 1. From the figure it can be observed that the diffraction peak has a symmetric shape, and its full width at half maximum (FWHM) is found to be about 135 arcsec using the Lorentz function to fit the measured data. The optical absorption properties have also been determined by optical transmission measurements in a wavelength range of 190–600 nm, and the wavelength dependence of optical transmittance is shown in Fig. 2. In principle, the optical transmittance should depend on the crystallinity and stoichiometry of films. The observation of oscillations in the

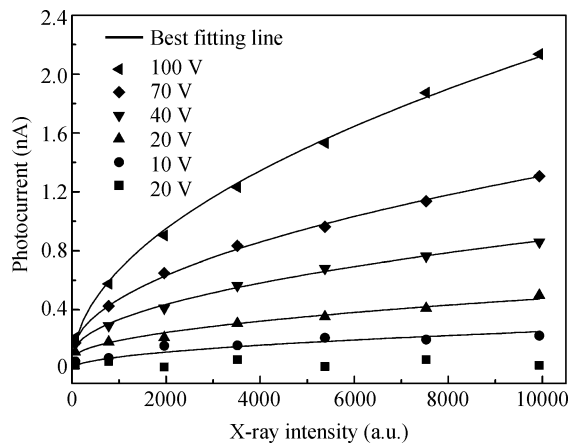


Fig. 3. Photocurrent of the AlN photoconductor versus the X-ray irradiation intensity at different applied voltages.

infrared and visible range, as well as a steep absorption edge around 200 nm, indicates that the AlN film has a smooth surface and high crystal quality. The band gap E_g is determined by the least-squares method using the Tauc equation^[6]:

$$(\alpha h\nu)^2 = A(h\nu - E_g), \quad (1)$$

where A is a constant, α is the absorption coefficient, and $h\nu$ is the photon energy. The best fitting results are also shown in the inset of Fig. 2, and the best-fitted value of the band gap is 6.17 eV, which is close to the bulk value of 6.2 eV. These results clearly suggest that the AlN film has a sufficient quality to be used to fabricate the photoconductors for X-ray detection.

In order to obtain the relationship between the photocurrent and the X-ray irradiation intensity for the AlN photoconductor, the dependence of X-ray irradiation intensity I on the current i flowing through the Cu anode X-ray tube, as well as the applied voltage V , is approximated by the following empirical equation^[7]:

$$I = Ai(V - V_0)^n, \quad (2)$$

where A is a constant, V_0 is the critical excitation voltage for characteristic rays, and n is the index. For the Cu anode X-ray tube used in the experiments, the values of V_0 and n are found to be about 8.6 kV and 1.6, respectively. The representative response of the AlN photoconductor to the X-ray irradiation intensity at different applied voltages is shown in Fig. 3. It can be observed that in the absence of X-ray irradiation the dark current is less than 0.1 nA at an applied voltage of 100 V, and under X-ray irradiation the photocurrent can reach values one order of magnitude higher than the dark current. It is surprising that the photocurrent increases nonlinearly as the X-ray irradiation intensity increases, and the dependence of the photocurrent I_{op} on the X-ray irradiation intensity can be fitted well by the following equation:

$$I_{op} = DI^{0.5}, \quad (3)$$

where D is a constant. The best fitting results are also shown in Fig. 3. This result clearly reveals that the photocurrent of the AlN photoconductor is proportional to the square root of X-ray irradiation intensity.

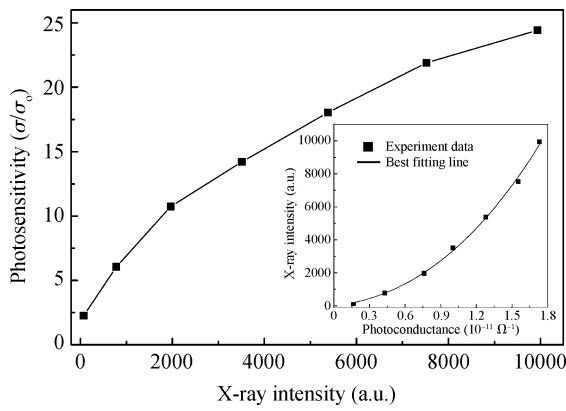


Fig. 4. Photosensitivity of AlN photoconductor as a function of X-ray irradiation intensity. The inset is the dependence of photoconductance on the X-ray irradiation intensity.

The photoconductance σ and intrinsic conductance σ_0 of the photoconductor is given by the following equations^[8]:

$$\sigma = e(\mu_e + \mu_h)n, \tag{4}$$

$$\sigma_0 = e\mu_e n_0, \tag{5}$$

where n is the excess carrier concentration, n_0 is the intrinsic carrier concentration, μ_e is the electron mobility, and μ_h is the hole mobility. Because in AlN the electron mobility is much larger than the hole mobility^[9, 10], the photosensitivity of the AlN photoconductor, i.e. the ratio of photoconductance to intrinsic conductance, can be expressed as:

$$\frac{\sigma}{\sigma_0} = \frac{n}{n_0}. \tag{6}$$

The equation clearly indicates that for the AlN photoconductor the ratio of excess carrier concentration to intrinsic carrier concentration is approximately equal to the photosensitivity. The photoconductance and intrinsic conductance of the AlN photoconductor are obtained from dark current and photocurrent–voltage characteristics, and the representative photosensitivity as a function of X-ray irradiation intensity is shown in Fig. 4. An inspection of the figure clearly reveals that in the whole range of X-ray irradiation intensity the photosensitivities are always significantly larger than one, i.e. the excess carrier concentrations are significantly larger than the intrinsic carrier concentrations according to Eq. (6). This implies that the carrier injection condition satisfies the high-level injection. Furthermore, it is well known that there are usually three carrier recombination mechanisms in semiconductors, i.e. direct recombination, Shockley–Read–Hall (SRH) recombination, and Auger recombination. The recombination mechanisms in the high-level injection can be described well by the ABC model, and the total carrier recombination rate U can be expressed by^[11]:

$$U = An + Bn^2 + Cn^3, \tag{7}$$

where A , B and C represent the SRH, direct and Auger recombination coefficients, respectively. The carrier generation rate G can be written as:

$$G = \beta I, \tag{8}$$

where β describes the number of carriers generated per unity X-ray irradiation intensity. In a steady state conditions, the carrier generation rate must be equal to the total carrier recombination rate, and using Eqs. (4), (7) and (8) the X-ray irradiation intensity I can be expressed in term of photoconductance σ :

$$I = A'\sigma + B'\sigma^2 + C'\sigma^3, \tag{9}$$

where A' , B' and C' are constants. The dependence of X-ray irradiation intensity on the photoconductance of the AlN photoconductor is shown in the inset of Fig. 4, and the fitting results obtained by the least square method using Eq. (9) are also presented. The best-fitted values are $A' = 814.5$, $B' = 2134.2$, and $C' = 379.1$. These results indicate that the carrier recombination in the AlN photoconductor is dominated by the direct recombination. The direct recombination rate is proportional to the square of carrier concentrations at a high-level injection, so it is expected that the photocurrent of the AlN photoconductor is proportional to the square root of the X-ray irradiation intensity, and its increase is getting slower with increasing the X-ray irradiation intensity. However, in the heteroepitaxial AlN film the edge dislocation density estimated by XRD measurements is found to be about $2.04 \times 10^{12} \text{ cm}^{-2}$, which is nearly two orders of magnitude higher than the screw dislocation density of $9.12 \times 10^6 \text{ cm}^{-2}$. This result clearly shows that the heteroepitaxial AlN film contains a large number of dislocations due to the lattice and thermal mismatch between the sapphire substrate and AlN film, and their main components are the edge dislocations. Therefore, the conclusion that the carrier recombination in the heteroepitaxial AlN film is not strongly affected by the dislocation defects can be obtained. In the GaN film the insensitivity of carrier recombination to the dislocation defects has been attributed to the lower dislocation electrical activity and small carrier diffusion length^[12]. The high temperature electrical conductivity measurement has been carried out in a temperature range of 600–900 K. The result reveals that the electrical properties of unintentionally doped AlN films are dominated by the residual V_N , and the trap level related to the dislocation defects is not observed. On the other hand, Taniyasu *et al.* have demonstrated that the dislocation defects can greatly degrade the electron mobility in the heteroepitaxial AlN film, and the electron mobility estimated for a typical dislocation density of 10^{11} cm^{-2} is well below $30 \text{ cm}^2/(\text{V}\cdot\text{s})$ at room temperature^[9, 10]. Furthermore, the reported hole mobility in a heteroepitaxial AlN film is very low, and its value is generally smaller than $15 \text{ cm}^2/(\text{V}\cdot\text{s})$ at room temperature^[10, 13]. According to Einstein's relationship between a diffusion constant and mobility, these results suggest that the carrier diffusion lengths in the heteroepitaxial AlN film are very small^[14]. Based on the above discussions, the insensitivity of the carrier recombination to dislocation defects in the heteroepitaxial AlN film can be attributed to the small carrier diffusion length.

Using the ABC model, the contribution from every recombination mechanism to the total recombination can be calculated as a function of X-ray irradiation intensity, and the results are presented in Fig. 5. From the figure it can be observed that the contribution from the Auger recombination increases slowly from 1% to 20% with an increase in X-ray irradiation intensity, and the contribution from the SRH decays exponentially from 70% to 15%. However, the contribution from the

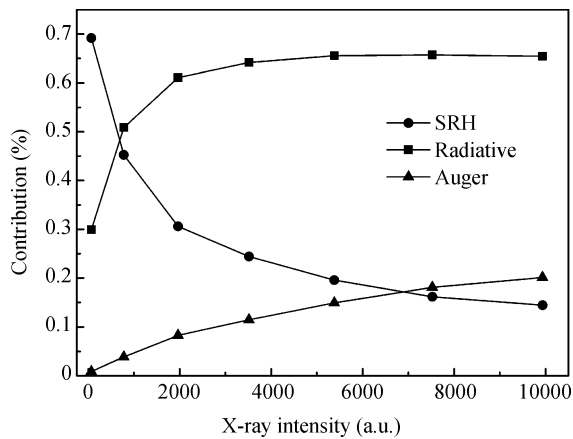


Fig. 5. Contribution from every recombination mechanism to the total recombination as a function of X-ray irradiation intensity.

direct recombination increases rapidly from 30% and quickly reaches the saturation value of 65% with an increase in X-ray irradiation intensity. These results imply that the main competition is between the direct recombination and the SRH recombination under the relatively weak X-ray irradiation intensity, and with an increase of X-ray irradiation intensity the competition between the SRH recombination and the Auger recombination dominates. However, the total contribution from the SRH and Auger recombination is greatly smaller than that from the direct recombination. This may be why the dependence of the measured photocurrent on the X-ray irradiation intensity can be fitted well by Eq. (2), as shown in Fig. 3.

4. Conclusions

In summary, we successfully demonstrate the feasibility of X-ray detection by using an AlN photoconductor, and its response to X-ray irradiation intensity is investigated in detail. The AlN film used to fabricate the AlN photoconductor has been characterized by XRD and transmittance spectra, and the results show that the FWHM of (0002) plane diffraction peak is 135 arcsec, and the band gap is 6.17 eV. The photocurrent measurements clearly reveal that in the absence of X-ray irradiation the dark current is less than 0.1 nA at an applied voltage of 100 V, and under X-ray irradiation the photocurrent can be

one order of magnitude larger than the dark current. Using the ABC model the direct recombination is found to dominate the carrier recombination in the AlN photoconductor, which is responsible for the dependence of the measured photocurrent on the square root of X-ray irradiation intensity.

References

- [1] Zhao H, Zou Z Y, Zhao W B, et al. Epitaxial growth of atomically flat AlN layers on sapphire substrate by metal organic chemical vapor deposition. *Chinese Journal of Semiconductors*, 2007, 28(10): 1568 (in Chinese)
- [2] Li W W, Zhao Y W, Dong Z Y, et al. Wet etching and infrared absorption of AlN bulk single crystals. *Journal of Semiconductors*, 2009, 30(7): 073002
- [3] Moscatelli F. Silicon carbide for UV, alpha, beta and X-ray detectors: results and perspectives. *Nucl Instr and Meth Phys Res A*, 2007, 583(1): 157
- [4] Owens A, Peacock A. Compound semiconductor radiation detectors. *Nucl Instr and Meth Phys Res A*, 2004, 531(1): 18
- [5] Bavdaz M, Peacock A, Owens A. Future space applications of compound semiconductor X-ray detectors. *Nucl Instr and Meth Phys Res A*, 2001, 458(1): 123
- [6] Zarwasch R, Rille E, Pulker H K. Fundamental optical absorption edge of reactively direct current magnetron sputter-deposited AlN thin films. *J Appl Phys*, 1992, 71(10): 5275
- [7] Hicks V. X-ray physics and X-ray tubes. *J Appl Phys*, 1941, 12(5): 364
- [8] Razeghi M, Rogalski A. Semiconductor ultraviolet detectors. *J Appl Phys*, 1996, 79(10): 7433
- [9] Taniyasu Y, Kasu M. Aluminum nitride deep-ultraviolet light-emitting p-n junction diodes. *Diamond & Related Materials*, 2008, 17(8): 1273
- [10] Taniyasu Y, Kasu M, Makimoto T. Increased electron mobility in n-type Si-doped AlN by reducing dislocation density. *Appl Phys Lett*, 2006, 89(18): 182112
- [11] David A, Grundmann M J. Droop in InGaN light-emitting diodes: a differential carrier lifetime analysis. *Appl Phys Lett*, 2010, 96(10): 103504
- [12] Lee S R, West A M, Allerman A A, et al. Effect of threading dislocations on the Bragg peakwidths of GaN, AlGaN, and AlN heterolayers. *Appl Phys Lett*, 2005, 86(24): 241904
- [13] Edwards J, Kawabe K, Stevens G, et al. Space charge conduction and electrical behaviour of aluminum nitride single crystals. *Solid-State Commun*, 1965, 3(6): 99
- [14] Rodenhausen H. Einstein's relation between diffusion constant and mobility for a diffusion model. *J Stat Phys*, 1989, 55(5): 1065